Epitope Mapping

Deutsche Ausgabe: DOI: 10.1002/ange.201501898
Internationale Ausgabe: DOI: 10.1002/anie.201501898

A Phosphorylation-Induced Turn Defines the Alzheimer's Disease AT8 Antibody Epitope on the Tau Protein**

*Neha S. Gandhi, Isabelle Landrieu, Cillian Byrne, Predrag Kukic, Laziza Amniai, François-Xavier Cantrelle, Jean-Michel Wieruszeski, Ricardo L. Mancera, Yves Jacquot, and Guy Lippens**

Abstract: *Post mortem biochemical staging of Alzheimer's disease is currently based on immunochemical analysis of brain slices with the AT8 antibody. The epitope of AT8 is described around the $pSer_{202}/pThr_{205}$ region of the hyperphosphorylated form of the neuronal protein tau. In this study, NMR spectroscopy was used to precisely map the AT8 epitope on phosphorylated tau, and derive its defining structural features by a combination of NMR analyses and molecular dynamics. A particular turn conformation is stabilized by a hydrogen bond of the phosphorylated Thr_{205} residue to the amide proton of Gly_{207}, and is further stabilized by the two Arg residues opposing the $pSer_{202}/pThr_{205}$.*

Alzheimer's disease (AD) is characterized by the emergence of two kinds of lesions: extracellular plaques that are composed of the amyloid β peptide (amyloid fibers),[1] and intraneuronal fibers that are composed of the hyperphosphorylated tau protein (neurofibrillary tangles).[2,3] The post mortem biochemical staging of the disease was initially based on Gallyas silver staining of brain slices,[4] however, a technically simpler approach based on immunochemistry has been proposed recently.[5] The antibody used for the labelling of the affected regions in the brain is the AT8 antibody, for which the epitope is centered on the $pSer_{202}/pThr_{205}$ region of the hyperphosphorylated (pathological) form of the protein tau.[6–8] Although this antibody recognizes the same phosphorylation pattern on foetal tau,[9] it has proven its value mainly in staining specifically the affected brain areas in AD patients, and it is also directly associated with neurofibrillary tangles in transgenic mouse models.[10] However, it is currently not well-known what epitope pattern this antibody exactly recognizes. In this study, we used an in vitro phosphorylation assay on full-length tau to perform epitope mapping of the AT8 antibody by NMR spectroscopy. NMR analysis of the resulting phosphorylated peptide in combination with scaled molecular dynamics (SMD[11]) indicated the existence of a distinct turn conformation, which is induced by the hydrogen bond between the phosphorylated side chain of $pThr_{205}$ and the amide proton of Gly_{207}. The turn is further stabilized by the electrostatic interactions between the $pSer_{202}/pThr_{205}$ side chains and Arg_{209}/Arg_{211}. Finally, we rationalized the precise location of the epitope in the primary sequence of tau441.

We used the recombinant CDK2/CycA3 kinase to phosphorylate a ^{15}N-labelled tau441 sample in vitro. The resulting phosphorylated tau was recognized both by the AT180 and AT8 antibodies.[12] Epitope mapping by NMR analysis confirmed the presence of the $pThr_{231}$ residue at the center of the AT180 recognition site.[13] The application of a similar approach by incubation with the AT8 antibody led to the disappearance of the resonances of $pThr_{205}$ and of Gly_{204}, its direct neighbor, and also of a previously unassigned resonance at 9.45 ppm (^1H NMR)/110.2 ppm (^{15}N NMR; Figure 1). The latter signal depends on the phosphorylation and has a ^{15}N NMR chemical shift characteristic of a glycine residue, but not of serine or threonine residue. When using Gsk3β as the modifying kinase, we had previously observed this outlying signal,[14] but it was absent when PKA kinase was used.[15] As the signal belongs to the AT8 epitope and hence should be located in the proline-rich region (PRR) of tau,[16] we produced a $^{13}C/^{15}N$-labelled tauF5 fragment (residues 165–245) that spans this PRR, phosphorylated it by CDK2/

[*] Dr. I. Landrieu,[+] Dr. L. Amniai, Dr. J.-F. Cantrelle, Dr. J.-M. Wieruszeski, Dr. G. Lippens
CNRS UMR 8576, University of Lille 1 (France)
E-mail: Guy.Lippens@univ-lille1.fr
Dr. N. S. Gandhi,[+] Dr. R. L. Mancera
School of Biomedical Sciences, CHIRI Biosciences
Curtin University, Perth (Australia)
Dr. C. Byrne, Dr. Y. Jacquot
CNRS UMR 7203, Université Pierre et Marie Curie
Ecole Normale Supérieure, Paris (France)
Dr. C. Byrne
Institut Baulieu, Kremlin-Bicêtre (France)
Dr. P. Kukic
Department of Chemistry, Cambridge University
Cambridge (UK)
[+] These authors contributed equally to this work.

[**] We thank Drs. J. Götz, B. Chambraud, and E. E. Baulieu for helpful discussion, and Dr. L. Peyriga for help with setting up the NMR experiments on the 800 MHz machine (LISBP, Toulouse, France). The 900 MHz NMR facility was supported by the CNRS (TGIR RMN THC, FR-3050, France), University of Lille 1, the European community (EDRF), and the Région Nord-Pas de Calais. Part of this work was financed by the ANR (program MALZ-TAF) and LabEx Distalz grant (France). The computational work was funded by a Curtin Early Research fellowship. This work was supported by resources provided by the Pawsey Supercomputing Centre with funding from the Australian Government and the Government of Western Australia.

Supporting information for this article (including the preparation of samples of proteins and phosphorylated peptides for NMR experiments, and details of the different NMR experiments and MD simulations) is available on the WWW under http://dx.doi.org/10.1002/anie.201501898.

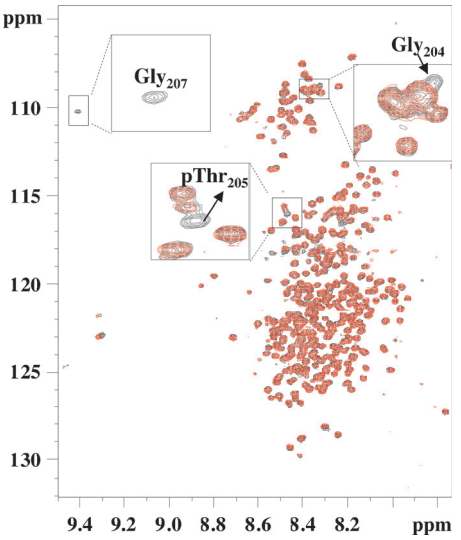

Figure 1. $^{1}H,^{15}N$ HSQC spectrum of tau441 phosphorylated by CDK2/CycA3 in the absence (black) or presence (red) of an equimolar concentration of AT8 antibody. The spectra were acquired at 293 K and 800 MHz.

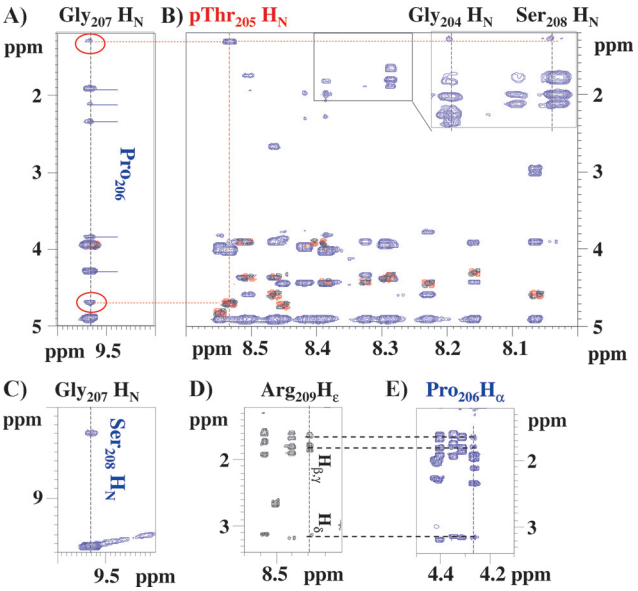

Figure 2. Homonuclear COSY (black/red) and NOESY (blue) spectra of peptide **1** at 287.4 K. A) The NOE interactions between the amide proton of Gly_{207} and the H atoms of $pThr_{205}$ are circled with red, whereas the NOE interactions with the ring of Pro_{206} are indicated by blue lines. B) When lowering the threshold in the insert, a weak NOE interaction between the methyl group of $pThr_{205}$ and the amide proton of Ser_{208} is observed. C) A strong NOE interaction between the amide protons of Gly_{207} and Ser_{208} indicates the turn conformation. D) TOCSY (black) spectrum of the side chains of the Arg residues in peptide **1**. E) NOESY (blue) spectrum of peptide **1** in D_2O showing the NOE interaction between Pro_{206} Hα and the side chain of Arg_{209}.

CycA3, and used triple-resonance spectroscopy to assign the different resonances (Figure S1 A,B; Table S1). On the basis of our observations, we assigned the outlying resonance to Gly_{207}. Its anomalous proton chemical shift directly depends on the phosphorylation state of Thr_{205}, as the signal disappears in the phosphorylated tau441 Thr_{205}Ala mutant (Figure S2). In order to remove all ambiguity, we produced a Gly_{207}Ala mutant of tau441, and again used CDK2/CycA3 to phosphorylate the resulting sample. Disappearance of the outlying signal (Figure S2) confirmed that the specific amide proton chemical shift belongs to Gly_{207}, and that it depends on the phosphorylation status of Thr_{205}.

The epitope defined by our NMR experiments confirms the central role of the $pThr_{205}$ residue. We then synthesized different phosphorylated peptides and used NMR spectroscopy to confirm that they reproduce the epitope in full-length tau. The spectrum of the Ac-GDRSGYSSPG-pS_{202}PGpT_{205}PGSRSRT-NH_2 peptide (peptide **1**; see Table S2 for a list of the peptides) reproduced the spectrum of the corresponding residues in tau441 well, including the signal of the amide proton at 9.53 ppm for the Gly_{207} residue (Figure 2; Figures S1–S3). The assignment of the peptide proton signals was based on homonuclear TOCSY/NOESY spectra (Figure S3, Table S3), and relied on the expected Hα(i-1)–H_N(i) NOE interactions. For the amide proton of Gly_{207}, we detected some additional medium- to long-range NOE interactions: with all ring protons of Pro_{206} (Figure 2 A), with the amide proton of Ser_{208} (Figure 2 C), and with the Hα/β and methyl protons of $pThr_{205}$ (Figure 2 A). When we contoured the spectrum at a lower threshold, but kept a mixing time of 200 ms, we also observed an NOE interaction between the amide proton of Ser_{208} and the methyl protons of $pThr_{205}$ (Figure 2 B). The NOE interaction between the side-chain protons of Arg_{209} and the Hα proton of Pro_{206} (Figure 2 D,E) further suggests a more compact conformation in this region. We then returned to the spectra of phosphorylated tauF5. The NOE interactions observed in peptide **1** were also observed in the NOESY-HSQC spectrum of phosphorylated tauF5 (Figure S1C), in agreement with the previous finding that peptide **1** can efficiently compete with tau in paired helical filaments for binding of the AT8 antibody.[8]

Molecular dynamics (MD) simulations can be used to probe the structure and dynamics of partially folded or unfolded proteins with the trajectories validated using back-calculated NMR parameters.[17] We recently employed MD simulations to probe the structural role of phosphorylation on the AT180 epitope of the tau(208–324) fragment.[18] The secondary structures induced by phosphorylation of the $pThr_{231}$ and $pSer_{235}$ residues obtained from the simulations and from the corresponding NMR measurements were in good agreement.[19] By applying a similar strategy, we generated a 1 μs trajectory for peptide **1** with phosphorylations at Ser_{202} and Thr_{205}. In contrast to what was found for other phosphorylated peptides of tau,[20] we observed no significant polyproline II (PPII) content in the secondary structure analyses of the trajectory (Figure S4). Because the outlying chemical shift of the Gly_{207} amide proton is expected to depend primarily on the Ψ angle of the preceding residue and on its own Φ angle,[21] we first clustered low-energy conformations into four zones defining these two torsional angles (Figure 3 A). The dominating cluster in the lower-left quadrant of the Ramachandran map ("well 1") contains 62 % of the conformers and corresponds to a helical turn con-

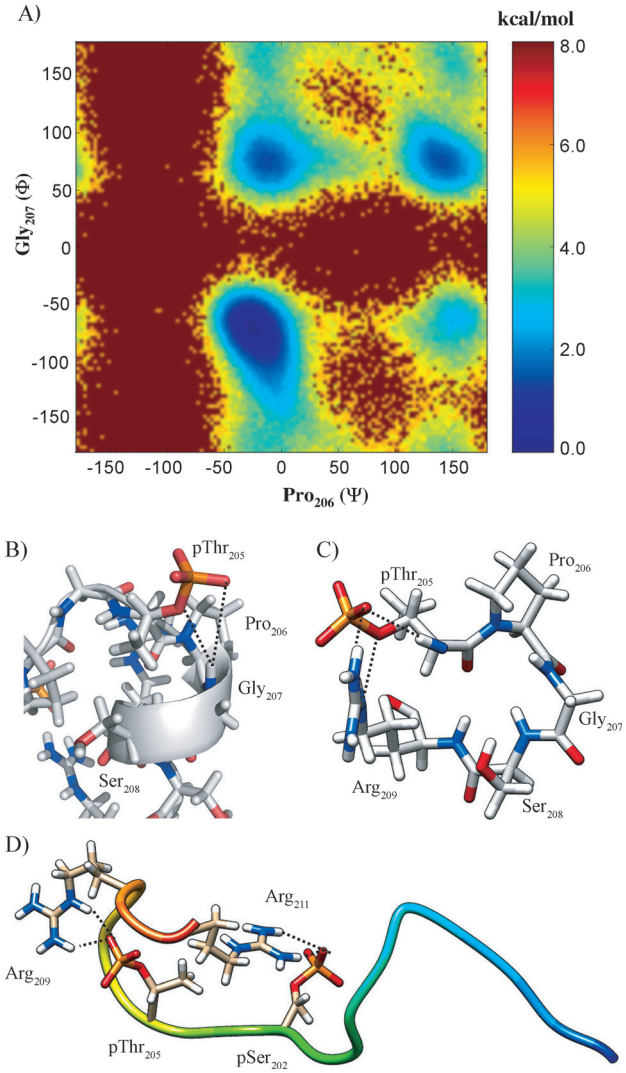

Figure 3. A) Low-energy conformations of the MD trajectory are clustered depending on the psi angle of Pro_{206} and the phi angle of Gly_{207}. Lowest to highest free energy (kcal mol^{-1}) from blue to red. The four clusters together with their representative structures are shown. The populations in the four clusters are as follows: "well 1" (lower left) 62.5%, "well 2" (lower right) 5%, "well 3" (upper right) 21%, "well 4" (upper left) 11.5%. B) Representative conformation of the turn conformation in well 1, with a $pThr_{205}(PO_3^-)$–Gly_{207}(HN) hydrogen bond. The turn is centered around Gly_{207}-Ser_{208} (proton–proton distance 2.5 Å), and positions the phosphate moiety on top of the amide proton of Gly_{207}. C) For part of the trajectory, an intra-residue $pThr_{205}$ (HN-PO_3^-) hydrogen bond is observed, but a salt bridge with the Arg_{209} side chain contributes to stabilizing the turn. D) $pSer_{202}$ contributes to the turn stability through its interaction with Arg_{211}. Hydrogen bonds are shown as black dotted lines.

formation that extends from Pro_{206} to Arg_{209} (Figure 3B). The phosphate group of $pThr_{205}$ contributes significantly to this conformation by engaging in a hydrogen bond with the amide proton of Gly_{207}. When we add the electrostatic contribution of the phosphate group on the amide proton chemical shift through the Buckingham equation[22] to the ShiftX2 CS prediction,[23] the average chemical shift of the different conformers in this well closely reproduces the experimental value of 9.5 ppm. Predicted chemical shifts for the conformers in the other sampled zones are significantly less in agreement with the experimental values (Table S4). The average distance between the amide protons of Gly_{207} and Ser_{208}, both central residues of the turn, is very short (< 2.9 Å) in well 1, in agreement with the strong NOE we observed in the NOESY spectrum of peptide **1** (Figure 2). When evaluating all other NOE constraints over the conformations of well 1, we found that the ensemble of the conformers characterized by this turn indeed satisfy all of them (Table S5). In the nonphosphorylated peptide **2**, the absence of NOE interactions between the Gly_{207}–Ser_{208} amide protons (Figure S5) further suggests that the pronounced interaction between the phosphate moiety of $pThr_{205}$ and the Gly_{207} amide proton is required to stabilize the turn conformation in the AT8-binding motif of peptide **1**.

When we analyzed the conformers in the most populated well in detail, we observed a dynamic exchange for the flanking residues of the turn. Even the phosphate group of $pThr_{205}$ is not anchored in a permanent manner to the Gly_{207} amide proton, and sometimes flips back to engage in a hydrogen bond with its own amide proton (Figure 3C), thereby reproducing the intra-residue hydrogen bond that was observed in model dipeptides incorporating a phosphorylated Thr residue.[24] In these conformers, though, the same $pThr_{205}$ group forms a salt bridge with the Arg_{209} side chain (Figure 3C), thereby maintaining the turn (Figure S6A) until the $pThr_{205}$ side chain flips back to the Gly_{207} amide proton (Figure S6B). When the phosphate group of $pThr_{205}$ is hydrogen bonded to the amide proton of Gly_{207}, the $pSer_{202}$ side chain further interacts with the Arg_{209} and/or Arg_{211} (Figure 3D). Although even further away than Arg_{209} from the phosphorylated residues, the amide proton of Arg_{211} indeed experiences an important downfield shift of 0.15 ppm between peptides **1** and **2** (Figure S7, Table S5). When only the Thr_{205} is phosphorylated, as in peptide **3**, amide protons of both Arg_{209} and Arg_{211} return partially toward their position in the nonphosphorylated peptide **2**, while the $pThr_{205}$ amide proton shifts 0.15 ppm downfield (Figure S7). The contribution of $pSer_{202}$ to the turn stability might therefore explain why both phosphorylation events are a prerequisite for the conformational epitope of the AT8 antibody.

Phosphorylation of the preceding Thr residue induces a similar turn by hydrogen bonding of the phosphate group to the glycine amide proton, thus skipping proline. This effect was very recently described for two motifs in the eIF4E binding 4E-BP2 protein, and is accompanied by the folding of a triple-stranded β sheet, thereby disrupting the binding of the central residues to eIF4E.[25] In the context of this triple-stranded β sheet, both turns are stable, with the Gly amide protons resonating around 11 ppm. A similar turn imposed by two antiparallel β strands without phosphorylation is also observed for the $P_{41}GSR_{44}$ tetrapeptide in the mycobacterial transcription factor CarD[20] (PDB code: 4L5G; Figure S8). In the case of the AT8 motif described here, however, there is no experimental evidence that the [$pSer_{202}$–Arg_{211}] peptide would adopt a similar β sheet conformation. Coupling constants, ^{13}C NMR chemical shifts (Table S3), and the absence of any interstrand NOE interactions all point toward the absence of a true β-sheet conformation for these residues. Without this β-sheet, the turn conformation is

not as rigid as in the eIF4E protein, in agreement with our SMD.

One might wonder why the pThr$_{205}$-Pro$_{206}$ motif is selectively recognized by the AT8 antibody, considering that ten Thr-Pro motifs occur in tau441, and that all are possible phosphorylation sites for the different proline-directed kinases. A closer look at the primary sequence of tau allows the grouping of these Thr-Pro motifs into three categories: those that have negatively charged residues directly downstream of Pro, those with a Thr-Pro-Pro motif, and those that have a neutral or positive charge at their C terminus (Figure 4). In

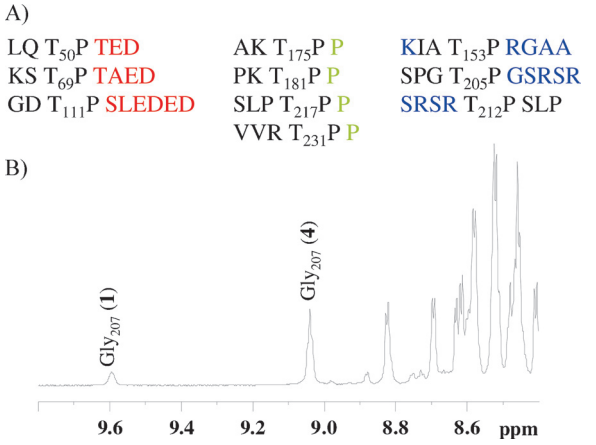

Figure 4. A) Thr-Pro motifs in the primary sequence of tau441 can be grouped in three categories. B) 1D spectrum of a 1:2 mixture of peptides **1** and **4** at pH 6.9, 287.4 K.

the third category, positive charges or neutral residues follow the Pro residue, but only the Thr$_{205}$-Pro$_{206}$ motif has a first positive charge separated by two flexible residues (Gly$_{207}$ and Ser$_{208}$). To investigate the role of the downstream charges, we synthetized peptide **4**, which is similar to peptide **1**, but with both Arg$_{209}$ and Arg$_{211}$ replaced by Glu (Table S2). As a result, the chemical shift of the Gly$_{207}$ amide proton decreases from 9.6 ppm to 9.0 ppm at pH 6.9 (Figure 4), whereas the chemical shift of the amide proton of pThr$_{205}$ increases from 8.6 ppm in peptide **1** to 8.9 ppm in peptide **4** (Figure S7). The negative charges introduced by both Glu$_{209}$ and Glu$_{211}$ hence disfavor the hydrogen bond of the phosphate of pThr$_{205}$ with the amide proton of Gly$_{207}$ and bias the conformation of pThr$_{205}$ to an intra-residue hydrogen bond. The presence of a flexible Gly and two positive charges downstream of the Pro-directed phosphorylation site together define the turn motif that is selectively recognized by the AT8 antibody, and suggest that it can only be generated at this exact position in the primary sequence of tau.

Previous studies employed Glu substitutions to mimic the phosphorylation at distinct positions without being hampered by a possible heterogeneous pattern of modifications and concluded an opening of the transient folding of tau.[26,27] However, these mutations did not lead to the pronounced shift of the Gly$_{207}$ amide proton,[27] further demonstrating that structural studies on experimentally phosphorylated proteins and substrates can lead to unexpected insights.[28] Here, we have structurally characterized the turn conformation induced by the phosphorylation of the tau441 Ser$_{202}$ and Thr$_{205}$ residues, in a motif that is selectively recognized by the AT8 antibody, which is specific for Alzheimer's disease. Whether and how the resulting turn in the intrinsically unstructured protein tau modifies its physiological and pathological aspects is now the topic of further studies.

Keywords: Alzheimer's disease · AT8 antibody · epitope mapping · phosphorylation · tau protein

How to cite: *Angew. Chem. Int. Ed.* **2015**, *54*, 6819–6823
Angew. Chem. **2015**, *127*, 6923–6927

[1] G. G. Glenner, C. W. Wong, *Biochem. Biophys. Res. Commun.* **1984**, *120*, 885–890.
[2] K. S. Kosik, C. L. Joachim, D. J. Selkoe, *Proc. Natl. Acad. Sci. USA* **1986**, *83*, 4044–4048.
[3] I. Grundke-Iqbal, K. Iqbal, Y. C. Tung, M. Quinlan, H. M. Wisniewski, L. I. Binder, *Proc. Natl. Acad. Sci. USA* **1986**, *83*, 4913–4917.
[4] H. Braak, E. Braak, *Acta Neuropathol.* **1991**, *82*, 239–259.
[5] H. Braak, I. Alafuzoff, T. Arzberger, H. Kretzschmar, K. Del Tredici, *Acta Neuropathol.* **2006**, *112*, 389–404.
[6] J. Biernat, E. M. Mandelkow, C. Schröter, B. Lichtenberg-Kraag, B. Steiner, B. Berling, H. Meyer, M. Mercken, A. Vandermeeren, M. Goedert, E. Mandelkow, *EMBO J.* **1992**, *11*, 1593–1597.
[7] M. Goedert, R. Jakes, E. Vanmechelen, *Neurosci. Lett.* **1995**, *189*, 167–169.
[8] R. Porzig, D. Singer, R. Hoffmann, *Biochem. Biophys. Res. Commun.* **2007**, *358*, 644–649.
[9] M. Goedert, R. Jakes, R. A. Crowther, J. Six, U. Lübke, M. Vandermeeren, P. Cras, J. Q. Trojanowski, V. M.-Y. Lee, *Proc. Natl. Acad. Sci. USA* **1993**, *90*, 5066–5070.
[10] F. Chen, D. David, A. Ferrari, J. Götz, *Curr. Drug Targets* **2004**, *5*, 503–515.
[11] W. Sinko, Y. Miao, C. A. F. de Oliveira, J. A. McCammon, *J. Phys. Chem. B* **2013**, *117*, 12759–12768.
[12] L. Amniai, P. Barbier, A. Sillen, J.-M. Wieruszeski, V. Peyrot, G. Lippens, I. Landrieu, *FASEB J.* **2009**, *23*, 1146–1152.
[13] L. Amniai, G. Lippens, I. Landrieu, *Biochem. Biophys. Res. Commun.* **2011**, *412*, 743–746.
[14] A. Leroy, I. Landrieu, I. Huvent, D. Legrand, B. Codeville, J.-M. Wieruszeski, G. Lippens, *J. Biol. Chem.* **2010**, *285*, 33435–33444.
[15] I. Landrieu, L. Lacosse, A. Leroy, J.-M. Wieruszeski, X. Trivelli, A. Sillen, N. Sibille, H. Schwalbe, K. Saxena, T. Langer, et al., *J. Am. Chem. Soc.* **2006**, *128*, 3575–3583.
[16] N. Gustke, B. Trinczek, J. Biernat, E. M. Mandelkow, E. Mandelkow, *Biochemistry* **1994**, *33*, 9511–9522.
[17] P. Robustelli, N. Trbovic, R. A. Friesner, A. G. Palmer, *J. Chem. Theory Comput.* **2013**, DOI: 10.1021/ct400654r.
[18] A. J. Lyons, N. S. Gandhi, R. L. Mancera, *Proteins* **2014**, DOI: 10.1002/prot.24544.
[19] N. Sibille, I. Huvent, C. Fauquant, D. Verdegem, L. Amniai, A. Leroy, J.-M. Wieruszeski, G. Lippens, I. Landrieu, *Proteins* **2011**, DOI: 10.1002/prot.23210.
[20] M. A. Brister, A. K. Pandey, A. A. Bielska, N. J. Zondlo, *J. Am. Chem. Soc.* **2014**, *136*, 3803–3816.
[21] D. S. Wishart, B. D. Sykes in *Methods in Enzymology* (Eds.: N. J. O. Thomas L. James), Academic Press, New York, **1994**, pp. 363–392.
[22] P. Kukic, D. Farrell, L. P. McIntosh, B. E. García-Moreno, K. S. Jensen, Z. Toleikis, K. Teilum, J. E. Nielsen, *J. Am. Chem. Soc.* **2013**, *135*, 16968–16976.
[23] B. Han, Y. Liu, S. W. Ginzinger, D. S. Wishart, *J. Biomol. NMR* **2011**, *50*, 43–57.

[24] K.-K. Lee, E. Kim, C. Joo, J. Song, H. Han, M. Cho, *J. Phys. Chem. B* **2008**, *112*, 16782 – 16787.
[25] A. Bah, R. M. Vernon, Z. Siddiqui, M. Krzeminski, R. Muhandiram, C. Zhao, N. Sonenberg, L. E. Kay, J. D. Forman-Kay, *Nature* **2014**, DOI: 10.1038/nature13999.
[26] S. Jeganathan, A. Hascher, S. Chinnathambi, J. Biernat, E.-M. Mandelkow, E. Mandelkow, *J. Biol. Chem.* **2008**, *283*, 32066 – 32076.
[27] S. Bibow, V. Ozenne, J. Biernat, M. Blackledge, E. Mandelkow, M. Zweckstetter, *J. Am. Chem. Soc.* **2011**, *133*, 15842 – 15845.
[28] L. N. Johnson, R. J. Lewis, *Chem. Rev.* **2001**, *101*, 2209 – 2242.

Received: March 2, 2015
Published online: April 16, 2015

